ISSN No:-2456-2165

Improving Thermal Performance of a Flat-plate Solar Collector by Applying TiO_2-Water Nanofluid

Siraj Ahmed
Libyan Authority for Scientific Research, Tripoli, Libya

Abstract:- In this work, the effect of titanium dioxide-water nanofluid on a flat-plate solar collector's performance has been studied. To obtain the nanofluid, we blended 2% TiO_2 (by mass) with pure water. To maintain the prepared nanofluid suspension's stability and to suppress the possible flocculation problem, we added 0.2% surface activator (Triton X-100) to the mixture by mass, which was further processed by continuous pulsing for 8 hours in an ultrasonic bath. EN ISO-9806 standard was followed for the experimental procedures. The mentioned process resulted in the formation of the required nanofluid and the comparative results are mentioned in the graphic form. The experiments conducted on a flat-plate solar collector showed 49.68% instantaneous enhancement for TiO_2-water nanofluid whereas, for pure water, it was only 36.20%.

Keywords:- *Flat-plate Solar Collector, Nanofluid, TiO_2-Water.*

I. INTRODUCTION

During recent years, interest in renewable energy sources has increased all over the world because fossil fuels are limited. Solar energy is now the most important renewable energy source and with passing time, its usage is increasing. Most solar systems have a solar collector and mechanisms for providing hot water but hot water-based solar collectors show low performance. Because of this problem, the research community is trying new methods to improve the solar collectors' performance.

In this context, the latest method is the use of nanoparticles or nanofluids for enhancing the solar collector's performance. Because of advancements in the material technology during the recent years, it is possible to obtain nano-sized metallic particles and add them to a fluid because they have high thermal conductivity; so the obtained nanofluid has more thermal conductivity as compared to conventional thermal transfer fluids. Consequently, they have a higher performance. Following are some basic physical factors, which considerably improve heat transfer through a nanofluid:

- Nano-sized solid metal is added to any of the basic fluids to form a suspension, which has a higher thermal conductivity as compared to that basic fluid.
- The thermal conductivity of fluid increases because nano-particles provide an increase in surface area for enhanced thermal transfer.
- A nanofluid has higher effective thermal capacity as compared to a base fluid.
- The fluid activity and thermal conductivity increase when turbulence volume increases.

In the literature, studies are generally relevant to thermo-physical properties [1-4] of different nanofluids [5-7]. Some researchers also focused on the performance of thermal systems, more specifically, heat pipes [8, 9]. Even now, the literature on nanofluid usage in solar collectors is very limited. Yousefi et al [10] experimentally studied the impact of changing nanofluids' pH. The nanofluid had 0.2% MWCNT (multi-walled carbon nanotubes), and it was applied in flat-plate solar collectors. Their work shows that nanofluids actually increase the collector performance, and more significantly at a low temperature. Yousefi et al conducted another study [11], in which they tried a 2% alumina nanofluid and Triton X-100 surface activator in a flat-plate solar collector. The nanofluid was maintained within 1-3 l/min. They reported a 28.3% increase in the collector performance. Lu et al [12] studied the nanofluids consisting of different CuO proportions in a vacuum-tube solar collector and tested its thermal performance. They observed that 1.2% CuO nanoparticle-water concentration provides the best thermal transfer. Nagarajan et al conducted a comprehensive study [13] on using nanofluids in solar collectors and analyzed their thermo-physical properties.

This work aims to test the effect of using TiO_2-water nanofluid in a flat-plate solar collector because so far, no study has been conducted on it. Experiments were conducted to determine the effect of TiO_2-water nanofluid, and the same experiment was repeated with pure water and then, the results were compared.

II. EXPERIMENTAL SETUP

Fig 1 shows the experimental setup, which has been prepared by following the EN ISO-9806 standard [14]. The experiment was conducted by first using pure water, and then TiO_2-water nanofluid. It is important to mention that aluminum was used to make the solar collector absorber plate, which was equipped with twelve parallel strips manufactured using the aluminum pipe-rolling method. Table 1 mentions the technical properties and dimensions of the solar collector.

ISSN No:-2456-2165

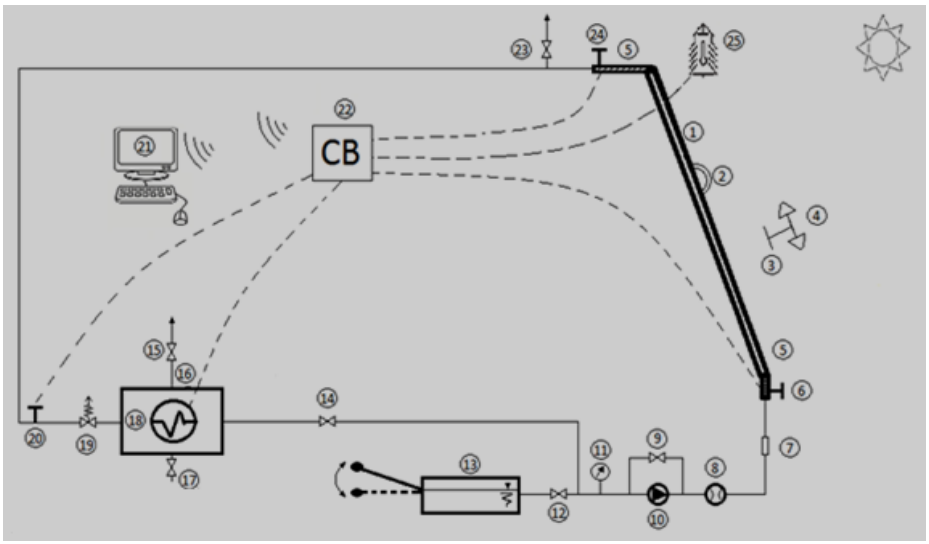

Fig. 1. Experimental setup

Key

1. Safety valve
2. Pyrgeometer
3. Pyranometer
4. Anemometer
5. Insulated pipe
6. Temperature sensor
7. Sight glass
8. Flow meter
9. Bypass valve
10. Pump
11. Manometer
12. Valve
13. Hydraulic hand pump
14. Valve
15. Drain valve
16. Nanofluid tank
17. Nanofluid drain valve
18. Heat exchanger
19. The flat plate solar collector
20. Temperature sensor (tank output)
21. Computer
22. Control panel
23. Air relief cock
24. Temperature sensor
25. Ambient air
26. temperature sensor

Table 1. Technical specifications of the flat-plate collector

Technical Features	
Width-length-thickness, cm	94x194x10
Gross area, m^2	1.91
Absorber	Aluminum
Absorber (net) area, m^2	1.60
Pipes, mm	13 pieces, Ø18
Collection pipe	¾ Ø
Weight, kg	35
Maximum pressure, bar	11
Operating pressure, bar	7
Maximum temperature, ºC	201
Flud capacity,L	3.5

It is essential to determine different input temperature performances to create the performance curves of a flat-plate solar collector; so, the collector's high input temperature performances are determined at low radiation. The experimental setup was equipped with an 8-liter tank following EN ISO-9806 standards and a 1.6kW heater. The main frame of the tank was manufactured using a heat insulation coating made of galvanized sheet of a 2mm alloy. For insulation, 5 cm thick glass wool was used that has 0.040W/mK heat transmission coefficient. To protect against the air leaks, the tank was coated with an aluminum foil. For maintaining the system circulation at a controlled flow rate, a flow meter Flomec OM Series and a Wilo-Stratos 25/1-6 pump were used. To assure 0.02 kg/s per square meter flow rate in the collector, a PID control system was used to monitor the pump and the flow meter. A general-purpose, high-speed, and accurate data acquisition and supervision card is used with an accurate PID pump control system. For measuring temperature and performance, K-type nickel-chromium thermocouples were tied at a distance of 200mm from the collector inlet and outlet following the EN ISO-9806 standard. PT-100 was used to measure the ambient temperature. A Class 1 pyranometer (Kipp & Zonen CMP 6) was used to measure the global shortwave radiation coming from the sun and sky, following the EN ISO-9060 standard. Table 2 shows the properties of the selected pyranometer, which is placed at the top of the collector with the same inclination angle (Fig. 2).

Table 2. Technical properties of a pyranometer

Spectral range (50% points)	286-2900
Sensitivity, µV/W/m²	5-20
Response time, s	18
Zero offset A, W/m²	<10
Zero offsets B, W/m²	< 4
Directional response (up to 80° with 1000 W/m² beam), W/m²	<20
Temperature dependence of sensitivity (-10 ºC to +40 ºC), %	< 4
Operational temperature range, °C	-40 to +90
Maximum solar irradiance, W/m²	2000
Field of view, °	190

ISSN No:-2456-2165

Fig 2. Position of the pyranometer

For data conversion and transferring the temperature, radiation, and flow rate values, an 18-bit transmitter card and a data converter were used.

III. NANOFLUID PREPARATION

To prepare the nanofluid, 97% pure nanoparticles with 44nm average size have been used. A blend of TiO_2 nanoparticles and water was prepared with 2% (mass/mass) concentration. To preserve the suspension stability, suppress possible flocculation (happens because of decreasing the contact angle and providing a wet outer surface), 0.2% Triton X-100 ((C14H22O (C2H4O)) was added. (Originally, Triton X-100 is the trademark of Rohm & Hass Co. and it was purchased from Down Chemical Company.) The surface activator was added to the mixture and the mixture was continuously pulsed for 8 hours in an ultrasonic bath for properly mixing it. Moreover, water in the bath was changed after regular intervals during the nanofluid preparation to prevent surface activator evaporation.

It was found that the prepared TiO_2-water nanofluid suspension was stable; it did not show flocculation problems either before or during the experiments. Then, three basic thermophysical properties of TiO_2-water nanofluid were determined, which include viscosity, specific heat capacity, and density. Table 3 shows the thermo-physical properties of TiO_2-water nanofluid:

Table 3. Thermo-physical properties of TiO_2-water nanofluid

Working fluid	Viscosity				Density (kg/m^3)	Specific Heat Capacity (kJ/kgK)
	20 ºC	40 ºC	60 ºC	80 ºC		
Pure water	0.98	0.64	0.45	0.35	998	4.18
TiO_2	1.01	0.92	0.67	0.54	1015	4.26

It is evident from Table 3 that the specific heat capacity increased by 0.08kJ/kgK when TiO_2-water nanofluid was used rather than using pure water. Moreover, it is also obvious that density and viscosity of TiO_2-water nanofluid are significantly higher than the pure water. Both viscosity and temperature of TiO_2 nanofluid increased, which shows that TiO_2 has better viscosity than pure water at any temperature. This happened because of metal particles in the nanofluid, which increased the mixture density. According to a previous study [15], the nanofluid density increases but it has the tendency to flocculate; therefore, low-density nanofluid is relatively more stable than the high-density nanofluid. Furthermore, a high temperature increases molecular vibration and speed, which increases thermal conductivity of the nanofluid and reduces its viscosity.

IV. EXPERIMENTAL PROCEDURE

To conduct this study, efforts were made to avoid all the problems, which can occur during the experiments. First, the experimental setup was tested using pure water. When the stability of the experimental setup was assured and results were obtained for pure water, it was decided to continue the experimental procedure with the nanofluid. The experiments were conducted at Ankara University, Turkey in an open area without any shade. Fig. 3 is the photo of the experimental setup. Using pure water in the solar collector, the first test was conducted. For experimental preparation, pure water was charged in the system using a hand pump to assure that no air is left in the system. The air, which existed in the system, was ejected using an air vent at the top of the collector's water inlet. This process was continued until the system pressure reached 4 bars. Thanks to the mechanism, it was possible to obtain sunlight at the right angle throughout the experiment, for which, the experimental setup was moved with hand in East-West and up-down direction. A sun-proof cover was used to cover the apparatus before starting the experiments. When the working fluid circulation pump automatically stepped in and the system provided the intended flow rate value, the experiments were initiated, for which, the cover on the collector was removed. It was noted that the radiation value reached 700W/m^2. The measured radiation, temperature, and flow rate values were transferred to the computer using an 18-bit data converter and transmitter card in the control panel. The experiments were completed when the solar radiation became less than 700W/m^2 and the collector inlet-outlet temperature difference was 1K (following ISO-9806 standard). The mentioned experiment was repeated a few times, and the maximum data was noted for the analysis.

When the experiments with pure water were over, the test system was completely discharged and the same procedure (charging and preparation) was repeated using TiO_2-water nanofluid. For comparative analysis, the tests were repeated using pure water for many times, and the highest values were selected.

ISSN No:-2456-2165

Fig. 3. Experimental Setup

V. THEORETICAL ANALYSIS

A. Thermal performance of a flat-plate solar collector

The collector used in closed-cycle experimental setup transfers the energy to the working fluid in the form of radiation, which is termed as instantaneous power and it is determined using the following equation [16]:

$$\dot{Q} = \dot{m}\, c_p\, \Delta T \quad (1)$$

Where,
$\dot{Q}$: Useful power extracted from the collector [W],
c_p: Specific heat capacity of working fluid [kJ/kgK],
$\dot{m}$: Mass flow rate of working fluid [kg/s],
ΔT: Inlet-outlet temperature difference (To-Tin) [K]

The collector's instantaneous thermal performance (η) has been calculated using the radiation that comes to a gross area of the collector and the instantaneous power ($\dot{Q}$) [16].

$$\eta = \frac{\dot{Q}}{I} \quad (2)$$

To calculate the incoming radiation, Equation 2 is used as follows considering the collector's gross area and the radiation coming to the unit's surface:

$$\eta = \frac{\dot{Q}}{A_G G} \quad (3)$$

Where,
G: Radiation intensity [W/m$^{2]}$
A_G: Gross area of the collector [m^2],

When radiation is low, the collector's inlet water temperature is increased with an electric heater, the performance curves graphically change according to the reduced temperatures (T_m^*). Fluid inlet temperature was increased with an electric heater to determine the collector's high inlet temperature under low radiation conditions, which shows that the working fluid collector's inlet temperature is semi-independent from radiation. The collector's instantaneous performance depends on working fluid inlet and outlet temperatures and radiation, which are independent of each other; so, it is essential to show performance changes through graphics according to reduced temperatures (T_m^*), which is stated in the following equations [16]:

$$T_m^* = \frac{(Tm - Ta)}{G} \quad (4)$$

Where,
T_m: Mean working fluid temperature [K],
T_m^*: Reduced temperature difference [m^{2}K/W],
T_a: Ambience temperature [K].

$$Tm = Tin + \frac{\Delta T}{2}$$

Where,
ΔT: Inlet and outlet temperature differences (To-Tin) [K]
T_{in}: Water temperature at collector inlet [K]

B. Mass flow rate of the working fluid

The working fluid's mass flow rate in collector ($\dot{m}$) is determined using the following equation [17]:

$$\dot{m} = 0.02\, A_G \quad (5)$$

Where,
A_G: Gross area of collector [m^2]
$\dot{m}$: Mass flow rate of working fluid [kg/s]

C. Uncertainty analysis

Using appropriate measuring devices, the data were obtained, and to assure validity of the experiments, precision level of the experimental setup was given extreme importance. For designing or planning experimental work, uncertainty analysis is considered as a very useful method. The most important parameters, which affect the accuracy, include the errors that occur during experiments; so, irrespective of the appropriateness of devices, uncertainty analysis is needed to deal with errors caused by test conditions, device selection, observation, environment, test plan, data reading, or port connection point. Equation 7 has been used for calculating the total uncertainty [18, 19].

$$W_S = \left[\left(\frac{\partial S}{\partial x_1} w_1\right)^2 + \left(\frac{\partial S}{\partial x_2} w_2\right)^2 + \ldots\ldots\ldots\ldots + \left(\frac{\partial S}{\partial x_n} w_n\right)^2\right]^{1/2} \quad (1)$$

Equation 7 determines the total uncertainty, which can occur, independent variable n, which affects the quantity S is given as x_1, x_2, x_3...x_n and S is the quantity which is necessary to be measured. The error rates for each independent variable and total uncertainty of quantity S are $w_{1,\ 2,\ 3,\ldots\ldots\ n}$ and W_s respectively. Table 2 shows the precisions, total uncertainty of measuring equipment, and technical properties.

ISSN No:-2456-2165

Table 2. Technical properties, precisions, and total uncertainty of the equipment

Measuring device	Measuring range	Precision	Total Uncertainty
Flow meter	0-2L/min	± %1	± %0.000125
Thermometer	0–120ºC	± 0.1ºC	± 0.075ºC
Pyranometer	0-2000W/m^2	± %1	± %1.41
Thermocouple	0-1200ºC	±0.1ºC	± %0.15
Anemometer (air velocity)	0–21m/s	±0.02m/s	± %0.012

VI. RESULTS AND DISCUSSION

Fig. 4 and 5 show the changes in working fluid inlet-outlet temperatures and the environment. It is obvious that the collector outlet temperature (To) closely follows the collector inlet temperature and it is always higher than Ti. Moreover, both inlet and outlet temperatures correspondingly increased. It happened because the collector outlet fluid was canalized towards the collector inlet because the experimental setup is a closed system, which was heated with an electric heater at low radiation. Collector inlet and outlet temperatures stabilized at 3 pm when their difference was almost 1K.

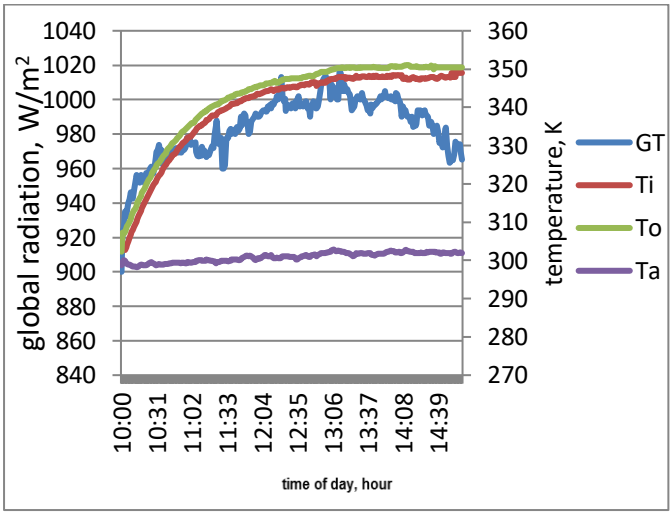

Fig. 4. Collector temperatures and radiation graphics for water

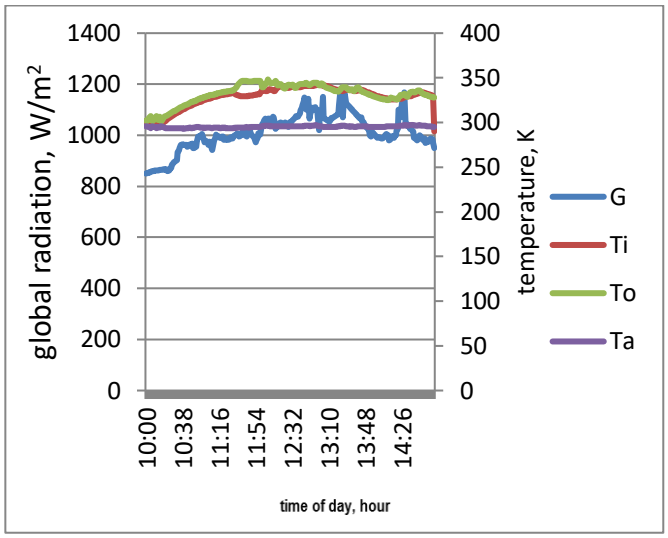

Fig. 5. Collector temperatures mean (TM) and power graphic for TiO_2-water nanofluid.

Fig. 5 shows that TiO_2-water nanofluid generated more energy as compared to pure water, which means that collector inlet and outlet temperatures reached higher temperatures at around 2pm when the nanofluid inlet and outlet temperatures were very close to each other. This can be explained by the fact that the nanofluid has high specific heat and less heat was lost between collector inlet and outlet.

For conducting the experiments, warmer days were selected when radiation values were more than 700W/m^2. For both experimental groups, the same collector is used, which has 1.65m^2 absorber plate. For experiments, the fluid circulation rate was maintained at 0.033 kg/s (±1%) (Eq. 5).

The average fluid temperature was determined for the experiments by taking the arithmetic mean of higher temperatures calculated at the flat-plate solar collector's inlet and outlet. Then the energy transfer to fluid reduced the temperature difference. The instantaneous thermal performance is calculated using Eq. 1, 3 and 4, respectively. Fig. 6 shows the performance variance graphic, which was generated based on the data obtained during the experiments with pure water and TiO_2-water nanofluid.

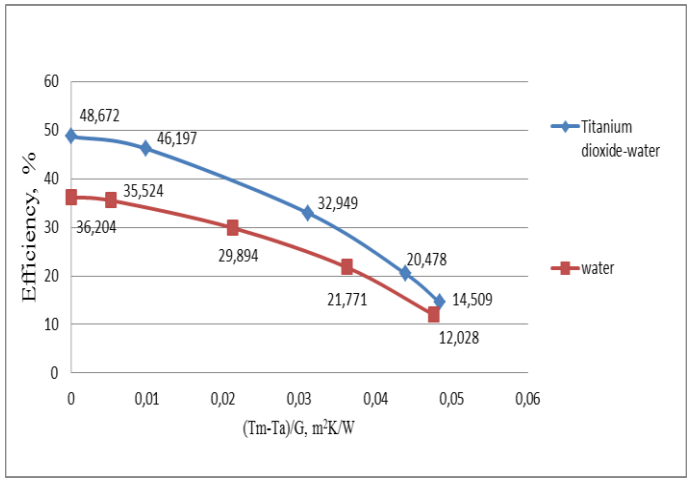

Fig. 6. Instantaneous performance reduced temperature difference for TiO_2-water

Fig. 6 also shows that when the temperature difference increases, the performance decreases because when the fluid temperature at collector inlet at low radiation increases, the collector inlet and outlet temperature difference reduces. Initially, the temperature of the fluid coming to the collector was equal to the ambient temperature; so, it was at the least heat throughout the experiments. At this point, the highest collector performance value was obtained. The performance curve shows a decreasing inclination because, as shown in Fig. 5 and 6, the radiation increased which reduced the collector inlet-outlet temperature difference and raised thermal leakage in the collector case, which depends on the increase in the collector temperature.

The polynomial equation $y = -8395.6x^2 – 105.02x + 36.204$ represents pure water. For pure water, when the reduced temperature difference is 0, the highest performance value was obtained, which was 36.204%. On the other hand, the polynomial equation $y = -11574x^2 – 141.34x + 48.672$ was obtained for the TiO_2-water nanofluid. In case, the reduced temperature difference is 0, the highest performance value was 48.67%. Thus, thermal performance of the flat-plate solar collector has shown 34.43% improvement, which is quite significant.

VII. CONCLUSION

In this research, TiO_2-water nanofluid was used as a working fluid in a flat-plate solar collector of a solar-powered hot water supplying system. It is clear from the experimental results that TiO_2-water nanofluid outperformed as compared to pure water. This happened because of an increase in working fluid contact surface and specific heat capacity for TiO_2-water nanofluid, which is 1.9% better as compared to pure water. Moreover instantaneous performance improvement in the collector output is 1.68-34.43% and in the useful heat drawn from the collector is 20.30-30.06%.

REFERENCES

[1]. Das S.K., Putra N, Thiesen P, Roetzel W. (2003). Temperature dependence of thermal conductivity enhancement for nanofluids. ASME Journal of Heat Transfer, 125: 567-574.
[2]. Patel HS, Das SK, Sundarajan T, Nair AS, George B, Predeep T. (2003). Thermal conductivity of naked and monolayer protected metal nanoparticles based nanofluids: Manifestation of anomalous enhancement and chemical effects. Applied Physics Letters, 83, 931-29.
[3]. Mahian O, Kianifar A, Kalogirou SA, Pop I, Wongwises S. (2013). A review of the applications of nanofluids in solar energy. Int J Heat Mass Transfer, 57, 582-94.
[4]. Xuan Y, Li Q. (2003). Investigation on convective heat transfer and flow features of nanofluids. Transactions of the ASME, Journal of Heat Transfer, 125, 151- 155.
[5]. Lee S, Choi US, Li S, Eastman JA, (1999). Measuring thermal conductivity of fluids containing oxide nanoparticles. Transactions of the ASME, Journal of Heat Transfer. 121, 280-289.
[6]. Zamzamian, A., KeyanpourRad, M., Kiani Neyestani, M., Jamal-Abad, M.T. (2014). An experimental study on the effect of Cu-synthesized/EG nanofluid on the efficiency of flat-plate solar collectors. Renewable Energy, 71, 658-664.
[7]. Eastman JA, Choi US, Li S, Thompson LJ, Lee S. (1997). Enhanced thermal conductivity through the development of nanofluids. Materials Research Society Symposium Proceedings. Materials Research Society, USA, 457: 3-11.
[8]. Sözen, A., Menlik, T., Gürü, M., Irmak, A.F., Kılıç, F., Aktaş, M. (2016). Utilization of Fly-ash Nanofluids in Two-Phase Closed Thermosyphon (TPCT) for Enhancing Heat Transfer, Experimental Heat Transfer, 29(3),337-354
[9]. Sözen, A., Menlik, T., Gürü, M., Boran, K., Kılıç, F., Aktaş, M., Çakır, M.T. (2016). A Comparative Investigation on The Effect Of Fly-Ash And Alumina Nanofluids on The Thermal Performance Of Two-Phase Closed Thermo-Syphon Heat Pipes, Applied Thermal Engineering, 96, 330-337.
[10]. Yousefi, T., Veisy, F., Shojaeizadeh, E., Zinadini, S., (2012). An experimental investigation on the effect of MWCNT-H_2O nanofluid on the efficiency of flat-plate solar collectors. Experimental Thermal and Fluid Science, 39, 207-212
[11]. Yousefi, T., Veysi, F. Shojaeizadeh, E., Zinadini, S., (2012). An experimental investigation on the effect of Al_2O_3-H_2O nanofluid on the efficiency of flat-plate solar collectors. Renewable Energy, 39, 293-298
[12]. Lu, L., Lıu, Z., Xıao, H., 2011. "Thermal performance of an open thermosyphon using nanofluids for high-temperature evacuated tubular solar collectors Part 1: Indoor experiment", Solar Energy, 85, 379–387
[13]. Nagarajan, P.K., Subramani, J., Suyambazhahan, S., Sathyamurthy, R., (2014). Nanofluids for solar collector applications: A Review. The 6th International Conference on Applied Energy – ICAE2014, 61, 2416-2434
[14]. International Standart ISO 9806, Solar energy-Solar thermal collectors-Test methods (2013)
[15]. X. Zhang, H. Gu, M. (2006). Fujii Effective thermal conductivity and thermal diffusivity of nanofluids containing spherical and cylindrical nanoparticles. Journal of Applied Physics. DOI: 10.1063/1.2259789.
[16]. Sowmy,D.S.,Ara,P.J.S.,Prado,R.T.A.,(2016) Uncertainties associated with solar collector efficiency test using an artificial solar simulator, Renewable Energy http://dx.doi.org/10.1016/j.renene.2016.08.054.
[17]. International Standart ISO 9806, Solar energy-Solar thermal collectors-Test methods (2013).
[18]. Holman, J.P., "Experimental Methods for Engineers", Sigapore: McGraw-Hill; 1994.
[19]. Aktaş, M., Şevik, S., Özdemir, M.B., Gönen, E., (2015). Performance analysis and modeling of a closed-loop heat pump dryer for bay leaves using artificial neural network. Applied Thermal Engineering, 87, 714-723.